Mutations of the Same Conserved Glutamate Residue in NBD2 of the Sulfonylurea Receptor 1 Subunit of the K_{ATP} Channel Can Result in Either Hyperinsulinism or Neonatal Diabetes

Roope Männikkö,[1] Sarah E. Flanagan,[2] Xiuli Sim,[1] David Segal,[3] Khalid Hussain,[4] Sian Ellard,[2] Andrew T. Hattersley,[2] and Frances M. Ashcroft[1]

OBJECTIVE—Two novel mutations (E1506D, E1506G) in the nucleotide-binding domain 2 (NBD2) of the ATP-sensitive K^+ channel (K_{ATP} channel) sulfonylurea receptor 1 (SUR1) subunit were detected heterozygously in patients with neonatal diabetes. A mutation at the same residue (E1506K) was previously shown to cause congenital hyperinsulinemia. We sought to understand why mutations at the same residue can cause either neonatal diabetes or hyperinsulinemia.

RESEARCH DESIGN AND METHODS—Neonatal diabetic patients were sequenced for mutations in *ABCC8* (SUR1) and *KCNJ11* (Kir6.2). Wild-type and mutant K_{ATP} channels were expressed in *Xenopus laevis* oocytes and studied with electrophysiological methods.

RESULTS—Oocytes expressing neonatal diabetes mutant channels had larger resting whole-cell K_{ATP} currents than wild-type, consistent with the patients' diabetes. Conversely, no E1506K currents were recorded at rest or after metabolic inhibition, as expected for a mutation causing hyperinsulinemia. K_{ATP} channels are activated by Mg-nucleotides (via SUR1) and blocked by ATP (via Kir6.2). All mutations decreased channel activation by MgADP but had little effect on MgATP activation, as assessed using an ATP-insensitive Kir6.2 subunit. Importantly, using wild-type Kir6.2, a 30-s preconditioning exposure to physiological MgATP concentrations (>300 μmol/L) caused a marked reduction in the ATP sensitivity of neonatal diabetic channels, a small decrease in that of wild-type channels, and no change for E1506K channels. This difference in MgATP inhibition may explain the difference in resting whole-cell currents found for the neonatal diabetes and hyperinsulinemia mutations.

CONCLUSIONS—Mutations in the same residue can cause either hyperinsulinemia or neonatal diabetes. Differentially altered nucleotide regulation by NBD2 of SUR1 can explain the respective clinical phenotypes. ***Diabetes*** **60:1813–1822, 2011**

From the [1]Henry Wellcome Centre for Gene Function, Department of Physiology, Anatomy and Genetics, University of Oxford, Oxford, U.K.; the [2]Institute of Biomedical and Clinical Research, Peninsula Medical School, Exeter, U.K.; the [3]Centre for Diabetes and Endocrinology, Houghton, Johannesburg, South Africa; and the [4]University College of London Institute of Child Health and Great Ormond Street Hospital, London, U.K.

Corresponding author: Frances M. Ashcroft, frances.ashcroft@dpag.ox.ac.uk.

Received 15 November 2010 and accepted 24 March 2011.

DOI: 10.2337/db10-1583

This article contains Supplementary Data online at http://diabetes.diabetesjournals.org/lookup/suppl/doi:10.2337/db10-1583/-/DC1.

The ATP-sensitive K^+ (K_{ATP}) channel plays a central role in glucose-stimulated insulin secretion from the pancreatic β-cell by linking the metabolic state of the cell to its electrical excitability (1–3). When plasma glucose levels rise, increased β-cell metabolism closes K_{ATP} channels, producing a membrane depolarization that opens voltage-dependent Ca^{2+} channels, increases Ca^{2+} influx, and triggers insulin release (4). Conversely, when plasma glucose levels fall, the decline in metabolism opens K_{ATP} channels, suppressing electrical activity and insulin secretion. As a consequence, mutations in the β-cell K_{ATP} channel lead to disorders of insulin secretion in humans and in animal models (5–11).

The β-cell K_{ATP} channel is a large macromolecular complex in which four inwardly rectifying potassium channel (Kir6.2) subunits form a central pore surrounded by four regulatory sulfonylurea receptor (SUR1) subunits (12,13). Both subunits are required for metabolic regulation of channel activity, which is mediated by changes in the intracellular concentrations of adenine nucleotides. Binding of ATP or ADP to Kir6.2 in an Mg-independent manner closes the channel, whereas interaction of Mg nucleotides with SUR1 enhances channel opening (14–17). The balance between these stimulatory and inhibitory effects determines the level of channel activity.

Gain-of-function mutations in the Kir6.2 or SUR1 subunits of the K_{ATP} channel are a common cause of neonatal diabetes, a rare inherited disorder characterized by the development of diabetes within the first 6 months of life (5–7). The diabetes may be permanent or follow a remitting–relapsing course (7). Fewer than 3% of patients experience DEND (developmental delay with epilepsy, muscle weakness and neonatal diabetes) syndrome; however, ≥20% manifest iDEND syndrome, an intermediate condition consisting of developmental delay, muscle hypotonia, and neonatal diabetes (6). Almost all mutations, whether in Kir6.2 or in SUR1, act by reducing the ability of ATP to close the channel, thereby enhancing the K_{ATP} current and preventing membrane depolarization when β-cell metabolism increases (5,6,11,18–22). Sulfonylurea drugs, which close K_{ATP} channels directly (23), stimulate insulin secretion in most patients with neonatal diabetes and have replaced insulin as the therapy of choice for this condition (22,24,25).

Loss-of-function mutations in Kir6.2 or SUR1 give rise to congenital hyperinsulinism, which is characterized by continuous and unregulated insulin secretion despite very

low plasma glucose levels (8,9,26,27). Patients usually present shortly after birth with persistent hypoglycemia that requires immediate treatment to avoid brain damage. Therapy in most cases involves a partial pancreatectomy, but less severe forms of the disease can be managed with the K_{ATP} channel-opener diazoxide.

Many disease-causing mutations in Kir6.2 and SUR1 have been described (3,7,18). However, to date, all mutations that cause neonatal diabetes have been identified in residues that differ from those that cause hyperinsulinemia. We describe here the identification and functional characterization of mutations at the same residue of SUR1 that can cause neonatal diabetes or its converse, hyperinsulinism.

SUR1 belongs to the family of ATP-binding cassette (ABC) transporters (28,29) and has 17 transmembrane helices arranged in groups of 5 (*N*-terminal transmembrane domain [TMD0]), 6 (TMD1), and 6 (TMD2). Two large cytosolic loops follow TMD1 and TMD2 and contain the nucleotide-binding domains (NBDs) that are characteristic of ABC proteins. Each NBD consists of a Walker A motif, a signature sequence, and a Walker B motif. The two NBDs are sandwiched in head-to-tail manner to form two closely linked nucleotide-binding sites (NBS) that comprise the signature sequence of one NBD and the Walker A and B motifs of the other (29).

The two NBS are not equivalent, however. Although both hydrolyze MgATP, NBS1 appears to have a higher affinity for MgATP and a lower rate of hydrolysis (30). It is also believed that the presence of MgADP at NBS2 is required to stimulate K_{ATP} channel activity (31). These differences may arise because NBS2 has the consensus sequence for ABC proteins, whereas that of NBS1 is degenerate; in particular, the Walker B motif of NBD2 is followed by a conserved catalytic glutamate residue (E1506), whereas the equivalent residue in NBD1 is an aspartate. This residue is critical in SUR1 function. In the closely related ABC transporter MRP1, swapping the catalytic carboxylates of the two NBDs transfers many of the properties of NBD1 to NBD2, and vice versa (32). Furthermore, the mutation of E1506 to lysine (E1506K) results in reduced channel activation by MgADP and is associated with hyperinsulinism (26,27). This article reports our investigation of how the mutation of E1506 to aspartate (E1506D) or glycine (E1506G) results in the opposite clinical condition of neonatal diabetes.

RESEARCH DESIGN AND METHODS

Mutation detection. Genomic DNA was extracted from peripheral leukocytes using standard procedures. The single-coding exon of *KCNJ11* and the 39 exons of *ABCC8* were amplified and sequenced as described (7). Reactions were analyzed on an ABI 3730 Capillary sequencer (Applied Biosystems, Warrington, U.K.). Sequences were compared with the reference sequences NM_000525 and NM_000352.2, which incorporate the alternatively spliced residue in exon 17 (L78208, L78224), using Mutation Surveyor 3.20 software (SoftGenetics, State College, PA). Mutation testing was performed on parental DNA extracted from peripheral leukocytes, and microsatellite analysis was used to confirm family relationships.

Molecular biology and oocyte preparation. Human Kir6.2 (Genbank NM000525; E23 and I337) and rat SUR1 (Genbank L40624) were used. Site-directed mutagenesis, synthesis of capped mRNA, and preparation of *Xenopus laevis* oocytes were performed as reported (33). Oocytes were co-injected with ~4 ng of wild-type or mutant SUR1 mRNA and ~0.8 ng Kir6.2 mRNA, incubated in Barth's solution and studied 1–4 days after injection. To simulate the heterozygous state, SUR1 was coexpressed with a 1:1 mixture of wild-type and mutant Kir6.2. For each batch of oocytes, all homomeric or heterozygous mutations were injected to enable direct comparison of their effects and to control for batch-to-batch variation in expression levels (see Supplementary Data).

Electrophysiology. Whole-cell currents were recorded using a two-electrode voltage clamp in response to voltage steps of ±20 mV from a holding potential of –10 mV, in a solution containing (in mmol/L) 90 KCl, 1 $MgCl_2$, 1.8 $CaCl_2$, and 5 HEPES (pH 7.4 with KOH) (33). Metabolic inhibition was induced by 3 mmol/L sodium azide, the K_{ATP} channel opener diazoxide (340 μmol/L) was used to fully activate the channels, and tolbutamide (0.5 mmol/L) was used to block K_{ATP} channels.

Macroscopic currents were recorded from giant inside-out patches at −60 mV; inward currents are shown as upward deflections of the current trace. The pipette (external) solution contained (in mmol/L) 140 KCl, 1.2 $MgCl_2$, 2.6 $CaCl_2$, and 10 HEPES (pH 7.4 with KOH). The intracellular solution contained (in mmol/L) 107 KCl, 11 EGTA, 2 $MgCl_2$, 1 $CaCl_2$, and 10 HEPES (pH 7.2 with KOH), as well as nucleotides as indicated. The Mg-free intracellular solution contained (in mmol/L) 107 KCl, 1 K_2SO_4, 10 EGTA, and 10 HEPES (pH 7.2 with KOH), as well as nucleotides as indicated.

ATP concentration-inhibition curves were constructed by alternating control and test solutions. To control for possible rundown, or activation by MgATP, the conductance in the test solution was expressed as the mean of that in control solution before and after nucleotide application. ATP concentration-response curves were fit with: $G/G_c = 1/\{1+[(ATP)/IC_{50}]^h\}$ (eq. 1), where (ATP) is the ATP concentration, IC_{50} is the ATP concentration at which inhibition is half maximal, and h is the slope factor.

In some experiments (Figs. 6 and 7), we used a conditioning prepulse of variable [MgATP], followed by a test pulse of MgATP. Current during the test pulse was expressed as a fraction of that in nucleotide-free solution.

Data are given as mean ± SEM. Significance was evaluated using the Student t test.

RESULTS

Patient characteristics and genetics. We identified novel heterozygous *ABCC8* mutations, E1507D (c.4521G>T) and E1507G (c.4520A>G), in two male probands. This numbering refers to the L78208 human *ABCC8* isoform that encodes 1,582 amino acids and contains an additional residue in NBD1; consequently, E1507 in our sequence is equivalent to E1506 in that of Huopio et al. (26,27).

Proband 1 with the E1507D mutation weighed 2.9 kg at birth (42 weeks' gestation) and was diagnosed as insulin-dependent at 10 weeks. At 30 weeks, the diabetes remitted and insulin treatment was withdrawn. The patient is currently 4 years old, and the diabetes remains in remission. Proband 2 weighed 3.5 kg at birth (40 weeks' gestation) and was diagnosed with diabetes at the age of 8 weeks. After an E1507G mutation was identified, the patient was successfully transferred from insulin to glibenclamide at the age of 6 months. He was treated with glibenclamide (2.5 mg, once daily) for ~4 months, at which time the diabetes remitted. The patient is currently 4 years old and remains in remission. A family history of diabetes had not been reported for either proband, and testing of parental samples demonstrated that the E1507D and E1507G mutations had each arisen de novo in the proband.

Effects on whole-cell K_{ATP} currents. We analyzed the effects of mutations at E1506 of rat SUR1 (equivalent to E1507 in the L78208 human *ABCC8* isoform) on the metabolic regulation of the K_{ATP} channel by measuring whole-cell currents. Wild-type (Kir6.2-SUR1) channels expressed in *Xenopus* oocytes are normally closed, due to the high intracellular ATP concentration ($[ATP]_i$), but can be opened by lowering $[ATP]_i$ using a metabolic inhibitor, such as sodium azide (Fig. 1). The subsequent addition of the K_{ATP} channel-opener diazoxide (0.34 mmol/L) increased the current only slightly, suggesting wild-type K_{ATP} channels are almost fully activated by 3 mmol/L sodium azide. Tolbutamide (0.5 mmol/L) almost completely blocked the current, confirming it flows through K_{ATP} channels.

Mutations that reduce the channel ATP sensitivity normally increase the whole-cell current in the absence of metabolic inhibition, reflecting the fact that they are less

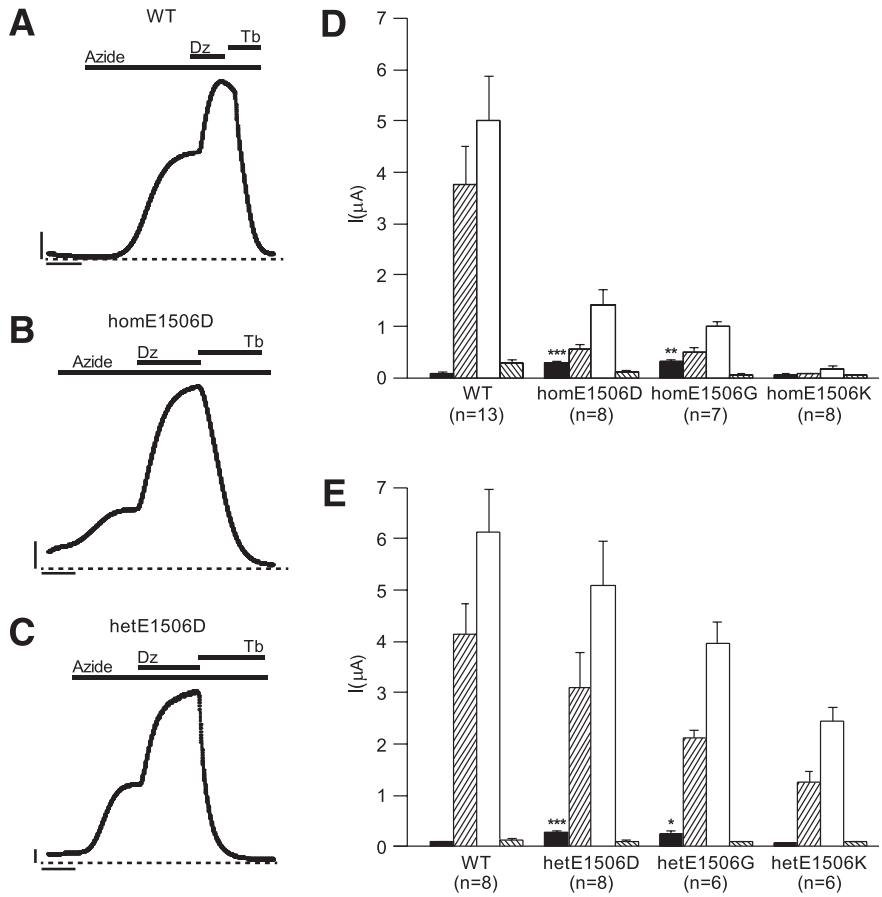

FIG. 1. Whole-cell K_{ATP} currents for wild-type and mutant channels. *A–C*: Representative whole-cell current amplitudes evoked by repeated voltage steps from −10 to −30 mV for wild-type (*A*, WT), and homomeric (*B*, homE1506D) or heterozygous (*C*, hetE1506D) Kir6.2/SUR1-E1506D channels. The bars indicate application of 3 mmol/L azide, 0.34 mmol/L diazoxide (Dz), and 0.5 mmol/L tolbutamide (Tb). The dashed line (- - -) indicates the zero current level. Scale bars are 0.5 μA (y-axis) and 400 s (x-axis). *D* and *E:* Mean steady-state whole-cell K_{ATP} current amplitudes for wild-type homomeric (*D*) and heterozygous (*E*) mutant channels. Currents were evoked by a voltage step from –10 to –30 mV before (control, ■) and after (▨) application of 3 mmol/L azide, in the presence of 3 mmol/L azide plus 0.34 mmol/L Dz (□), and 3 azide + 0.5 mmol/L Tb (▧) for WT and SUR1 mutant channels, as indicated. The number of oocytes tested is given *below the bars*. *$P \leq 0.05$, **$P \leq 0.01$, ***$P \leq 0.001$ against WT (Student *t* test). The error bars show the SEM.

blocked by resting $[ATP]_i$. A small but significant increase in resting current was observed for both homomeric Kir6.2/SUR1-E1506D (homE1506D) and Kir6.2/SUR1-E1506G (homE1506G) channels (Fig. 1). These currents were only slightly enhanced by metabolic inhibition but were further increased by diazoxide, suggesting azide-induced changes in nucleotide concentrations may be insufficient to fully activate the mutant channels. As previously reported (27), Kir6.2/SUR1-E1506K (homE1506K) currents were minimal in both the absence and presence of azide but were slightly increased by diazoxide. All mutant channels were strongly blocked by tolbutamide.

The resting currents of heterozygous (het) E1506D and hetE1506G channels were significantly greater than wild-type channels, which may explain why these mutations cause neonatal diabetes. Azide strongly activated all heterozygous channels, and in the additional presence of diazoxide there was a further increase. The maximal hetE1506D current was not significantly different from the wild-type current, and that of het1506G channels was only slightly smaller. These results suggest that hetE1506D and hetE1506G channels retain metabolic sensitivity and that their functional expression is similar to wild-type channels. The maximal amplitude of hetE1506K channels was reduced, as previously reported (27).

Tolbutamide (500 μmol/L) blocked hetE1506D currents by 95 ± 1% (n = 8), hetE1506G currents by 95 ± 1% (n = 6), and E1506K currents by 91 ± 2% (n = 6) compared with 96 ± 1% (n = 7) for wild-type channels.

Effects on K_{ATP} channel ATP sensitivity. In the cell-attached configuration, the homE1506D and homE1506G currents were both larger than wild-type or homE1506K currents, consistent with the whole-cell resting currents (Supplementary Fig. 2*A*). However, no significant difference was found between wild-type and mutant hetE1506 channels.

There was no difference in the amplitude of wild-type and homE1506K K_{ATP} currents recorded after patch excision (Table 1, Supplementary Fig. 2*B*), indicating the smaller amplitude of homE1506K whole-cell currents is not attributable to reduced channel expression. In contrast, homE1506D and homE1506G currents were both substantially smaller. However, there was no difference in hetE1506G currents and a <50% decrease in het1506D currents (Table 1, Supplementary Fig. 2*B*). This suggests that the neonatal diabetes mutations have little (E1506D) or no (E1506G) effect on expression levels of the K_{ATP} channel in the heterozygous state. To determine the molecular mechanism of action of E1506 mutations, we studied homomeric channels because the single population of channels simplifies the analysis.

TABLE 1
ATP sensitivity of wild-type and mutant channels

Clone	Excised patch current (nA)	n	Preincubation with zero ATP: IC_{50} Mg^{2+}-free ATP (μmol/L)	n	Preincubation with zero ATP: IC_{50} MgATP (μmol/L)	n	Preincubation with zero ATP: % Current in 100 μmol/L MgATP	Preincubation with 10 mmol/L MgATP: IC_{50} MgATP (μmol/L)	n	Preincubation with 10 mmol/L MgATP: % Current in 100 μmol/L MgATP
SUR1	13.1 ± 0.8	145	8.6 ± 1.1	7	13.1 ± 0.9	23	11 ± 1	30 ± 3	11	20 ± 2
homE1506D	4.0 ± 0.4*	96	8.8 ± 1.0	7	20.6 ± 1.5*	11	18 ± 2†	78 ± 3*	8	42 ± 2*
homE1506G	1.9 ± 0.2*	79	7.0 ± 1.4	7	19.0 ± 1.5†	10	16 ± 1†	108 ± 10*	7	51 ± 4*
homE1506K	14.2 ± 1.2	66	6.9 ± 1.2	7	11.5 ± 0.9	11	8 ± 1	18.1 ± 1.4†	7	8 ± 1*
hetE1506D	7.5 ± 1.7‡	13						48 ± 5†	9	28 ± 2‡
hetE1506G	11.2 ± 2.6	10						47 ± 5†	7	26 ± 3
hetE1506K	12.6 ± 3.0	6						26 ± 1	5	13 ± 1‡

Data are mean ± SEM; n = number of patches. Excised patch currents were measured immediately after excision into nucleotide-free solution
*$P \leq 0.001$, †$P \leq 0.01$, ‡$P \leq 0.05$, all against wild type (Student t test).

There was a slight reduction in MgATP block for homE1506D and homE1506G channels but no effect for homE1506K channels (Fig. 2*A–D*); the concentration of ATP producing half-maximal inhibition (IC_{50}) was 21 μmol/L for homE1506D, 19 μmol/L for homE1506G, 12 μmol/L for homE1506K, and 13 μmol/L for wild-type (E1506) channels (Table 1). The reduced ATP sensitivity of neonatal diabetes channels may account for the increased resting whole-cell currents produced by these mutations.

We next analyzed the ATP sensitivity in the absence of Mg^{2+}. This allows the effects of a mutation on ATP inhibition at Kir6.2 to be isolated from its action on Mg-nucleotide

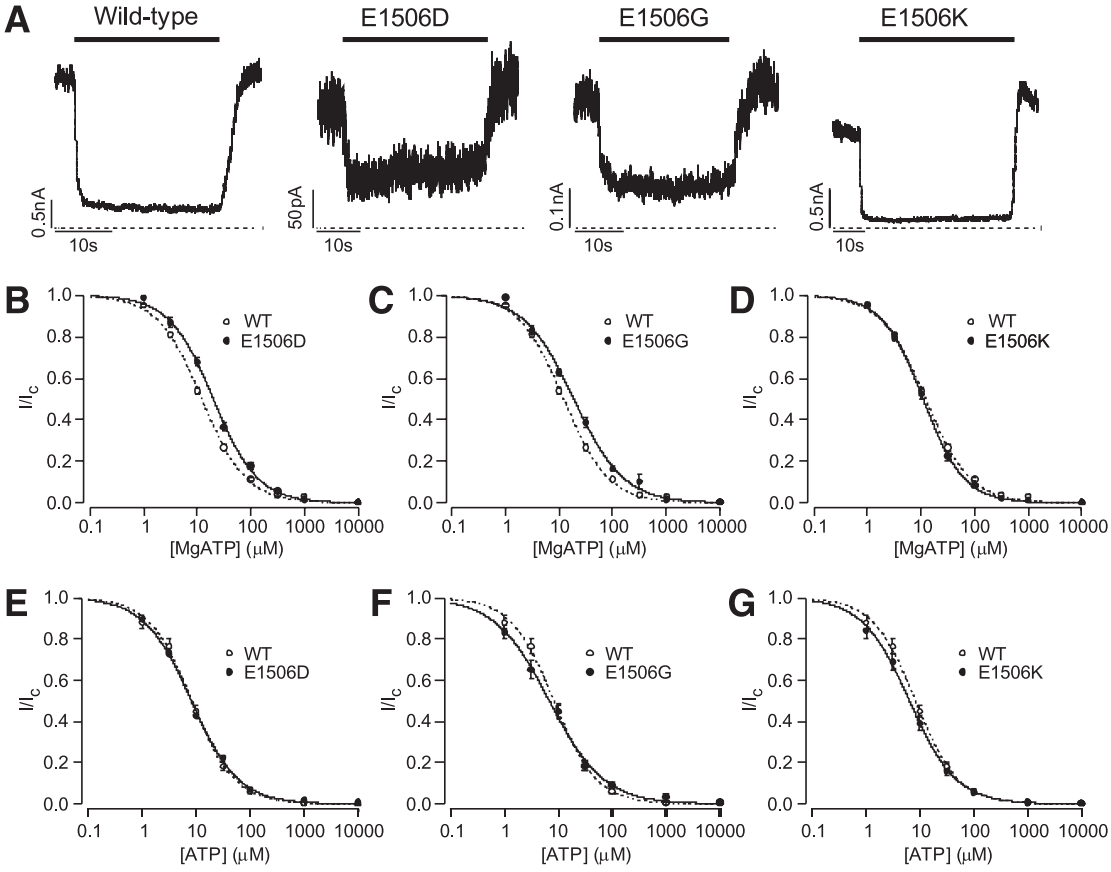

FIG. 2. ATP sensitivity of wild-type (WT) and mutant channels. *A*: Representative inside-out patch currents recorded in response to MgATP (100 μmol/L) for channels composed of WT Kir6.2 and WT or mutant SUR1, as indicated. The dashed lines (- - -) indicate the zero-current level. The solid lines (——) indicate nucleotide application. *B*: Mean relationship between K_{ATP} current (I), expressed relative to that in the absence of nucleotide (I_c), and ATP concentration in the presence (*B–D*) or absence (*E–G*) of 2 mmol/L Mg^{2+} for WT (○, - - -) and mutant (●, ——) channels. The lines are drawn to eq. 1, with the following parameters (in μmol/L for IC_{50}): *B–D*: wild-type (n = 23), IC_{50} = 12.2, h = 1.05; *E–G*: WT (n = 7), IC_{50} = 8.3, h = 1.09. *B*: Kir6.2/SUR1-E1506D (n = 11), IC_{50} = 20.1, h = 1.05. *C*: Kir6.2/SUR1-E1506G (n = 10), IC_{50} = 18.8, h = 0.93. *D*: Kir6.2/SUR1-E1506K (n = 11), IC_{50} = 11.0, h = 1.14. *E*: Kir6.2/SUR1-E1506D (n = 7), IC_{50} = 8.2, h = 1.00. *F*: Kir6.2/SUR1-E1506G (n = 7), IC_{50} = 6.9, h = 0.86. *G*: SUR1-E1506K (n = 7), IC_{50} = 6.4, h = 1.00.

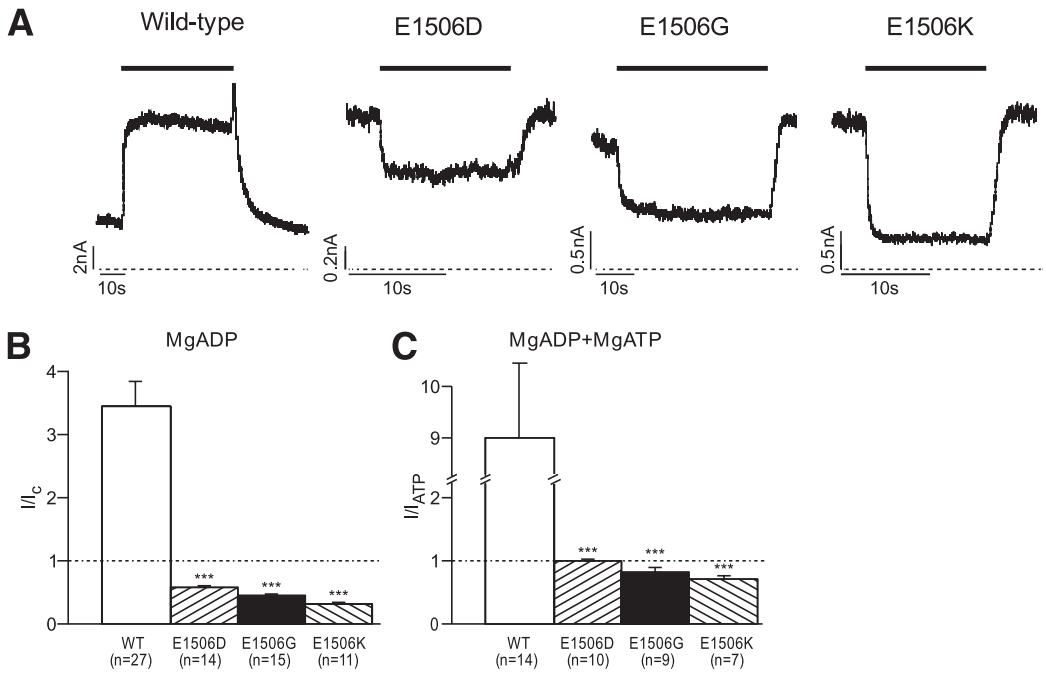

FIG. 3. MgADP activation of wild-type (WT) and mutant channels. *A*: Representative inside-out patch currents recorded in response to application of MgADP (100 μmol/L) for channels composed of WT Kir6.2 and WT or mutant SUR1, as indicated. The dashed lines (- - -) indicate the zero-current level. The solid bars (■) indicate the application of nucleotide. Note that 100 μmol/L MgADP activates WT-SUR1 channels but blocks all the mutant E1506 channels. *B* and *C*: MgADP activation of WT or mutant Kir6.2/SUR1-E1506 channels, as indicated. The number of patches is indicated *below the bars*. *B*: K_{ATP} current (I) in the presence of 100 μmol/L MgADP is expressed relative to the current in the absence of nucleotides (I_C). *C*: K_{ATP} current (I) in the presence of 100 μmol/L MgADP and 100 μmol/L MgATP is expressed relative to the current in the presence of 100 μmol/L MgATP alone (I_{ATP}). *$P \le 0.05$, **$P \le 0.01$, ***$P \le 0.001$ against wild type (Student *t* test). Statistical significance between mutant E1506 channels is reported in Supplementary Table 1. The error bars show the SEM.

stimulation at SUR1 because ATP does not interact with SUR1 in the absence of Mg^{2+} (34). None of the homE1506 mutant channels showed changes in ATP sensitivity in the absence of Mg^{2+} (Fig. 2*E–G*, Table 1), suggesting that the altered MgATP sensitivity of the homE1506D and homE1506G channels is not a consequence of a reduced ATP block at Kir6.2 but may arise from enhanced Mg-nucleotide activation at SUR1.

The lack of an effect of the homE1506K mutation on channel inhibition by ATP is in agreement with previous studies (27).

Effects on MgADP activation of K_{ATP} channel. We next examined Mg-nucleotide activation of wild-type and mutant channels. As is well established, K_{ATP} currents decline in amplitude after patch excision into nucleotide-free solution (35). Application of 100 μmol/L MgADP reversed this run-down and stimulated channel activity. Activation was quantified by expressing the current in the presence of MgADP as a fraction of that in the control solution before nucleotide application.

Wild-type K_{ATP} currents were increased ~3.5-fold by 100 μmol/L MgADP (Fig. 3*A* and *B*). By contrast, MgADP blocked all three mutant channels: by 77% for homE1506K, 55% for homE1506D, and 42% for homE1506G channels. Qualitatively similar results were observed in the presence of 100 μmol/L MgATP (Fig. 3*C*). The inability of MgADP to

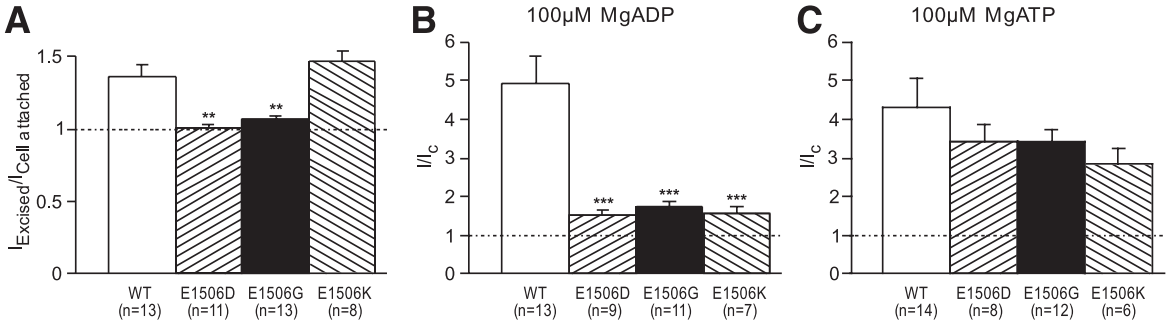

FIG. 4. MgADP and MgATP activation of SUR1-E1506 mutations on a Kir6.2-G334D background. MgADP and MgATP activation of K_{ATP} channels composed of Kir6.2-G334D and WT or mutant SUR1, as indicated. The number of patches is indicated *below the bars*. *A*: The maximal K_{ATP} current after patch excision is expressed relative to that in the cell-attached patch. K_{ATP} current (I) in the presence of 100 μmol/L MgADP (*B*) or 100 μmol/L MgATP (*C*) is expressed relative to the current in the absence of nucleotides (I_C). *$P \le 0.05$, **$P \le 0.01$, ***$P \le 0.001$ against wild type (Student *t* test). Statistical significance between mutant E1506 channels is reported in Supplementary Table 1. The error bars show the SEM.

activate the homE1506K channels in the presence or absence of ATP has been reported previously (27) and probably underlies the failure of these channels to open upon metabolic inhibition.

Previous studies have shown that in the absence of Mg^{2+}, 100 μmol/L ADP blocks wild-type K_{ATP} channels by ~60% (16) by binding to the inhibitory site on Kir6.2. The fact that homE1506D and homE1506G channels were blocked <60% by 100 μmol/L MgADP suggests that MgADP may retain some small stimulatory effect on these channels but that this is masked by inhibition at Kir6.2. To assess if this is correct, we examined the effect of MgADP on a Kir6.2-G334D background. The G334D mutation abolishes block by ATP (36) and thus allows the effects of Mg-nucleotides on SUR1 to be studied in isolation from their effects at Kir6.2.

Effects of MgATP and MgADP activation on E1506 mutants expressed on the Kir6.2-G334D background. Kir6.2-G334D/SUR1 (G334D/E1506) channels were highly active in the on-cell configuration (Fig. 4*A*) and the currents increased 1.4-fold on patch excision. No increase in current was observed for the Kir6.2-G334D/SUR1-E1506D (G334D/E1506D) or Kir6.2-G334D/SUR1-E1506G (G334D/E1506G) channels; in contrast, the Kir6.2-G334D/SUR1-E1506K (G334D/E1506K) currents increased 1.5-fold on excision. This suggests that the G334D/E1506 and G334D/E1506K channels were partially blocked under resting conditions in the oocyte, whereas the G334D/E1506D and G334D/E1506G channels were fully open. Larger amplitudes were found for the G334D/E1506 (8.5 ± 1.9 nA, n = 16) and G334D/E1506K (14 ± 1.9 nA, n = 9) currents than for the G334D/E1506D (1.0 ± 0.2 nA, n = 11) or G334D/E1506G (0.8 ± 0.2 nA, n = 13) currents, again suggesting that the E1506D and E1506G mutations may impair surface expression in the homomeric state.

MgADP (100 μmol/L) activated G334D/E1506 channels approximately fivefold (Fig. 4*B*, Supplementary Fig. 1). Its greater efficacy compared with Kir6.2/SUR1 channels (~3.5-fold, Fig. 3) presumably reflects a lack of MgADP block at Kir6.2 when G334 is mutated. Activation of E1506 mutant channels was greatly reduced, but not completely

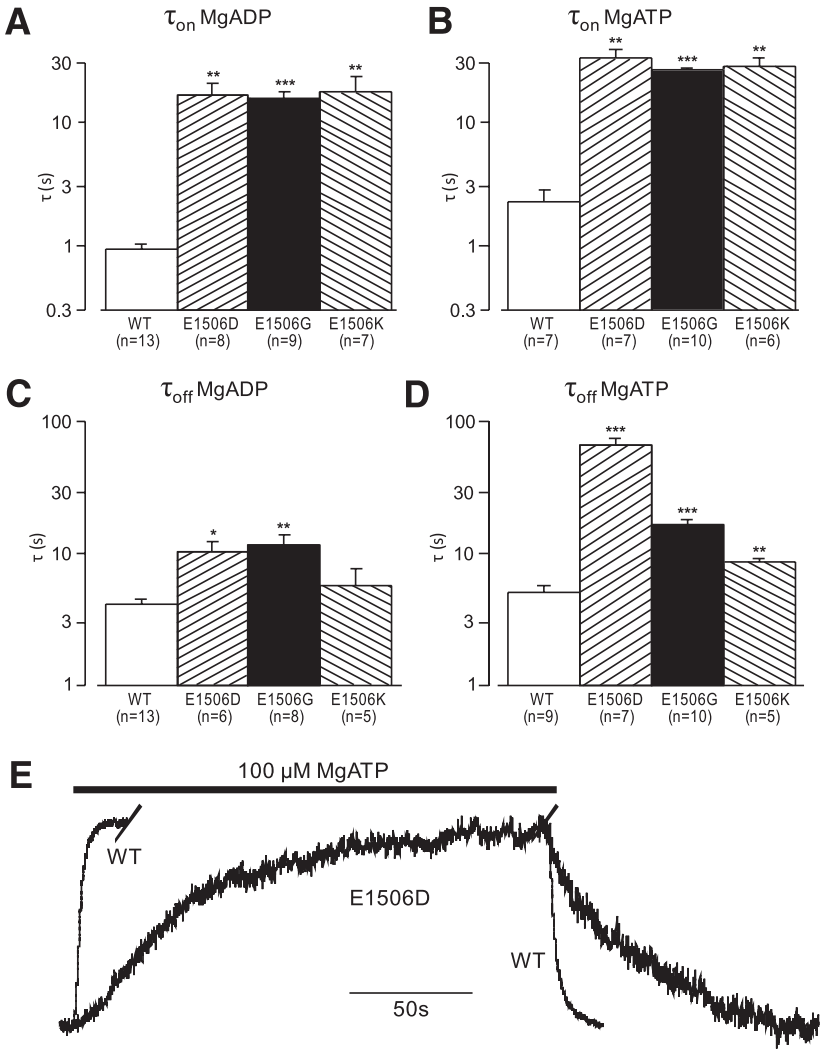

FIG. 5. Time course of MgADP and MgATP activation of K_{ATP} channels. Channels were composed of Kir6.2-G334D and wild-type (WT) or mutant SUR1 subunits, as indicated. Current activation and deactivation were fit with a single exponential function. The number of patches is indicated *below the bars*. Time constant of current activation (τ_{on}) by 100 μmol/L MgADP (*A*) or 100 μmol/L MgATP (*B*) is shown. Time constant of current deactivation (τ_{off}) after removal of 100 μmol/L MgADP (*C*) or 100 μmol/L MgATP (*D*) is shown. *$P \le 0.05$ **$P \le 0.01$, ***$P \le 0.001$ against wild-type, (Student *t* test). Statistical significance between mutant E1506 channels is reported in Supplementary Table 1. The error bars show the SEM. *E*: Representative current traces for WT and Kir6.2/SUR1-E1506D (E1506D) channels. The horizontal bar indicates the duration of application of 100 μmol/L MgATP. The WT trace is interrupted to align the time point of ATP removal with that of the E1506D trace. Current amplitudes are normalized.

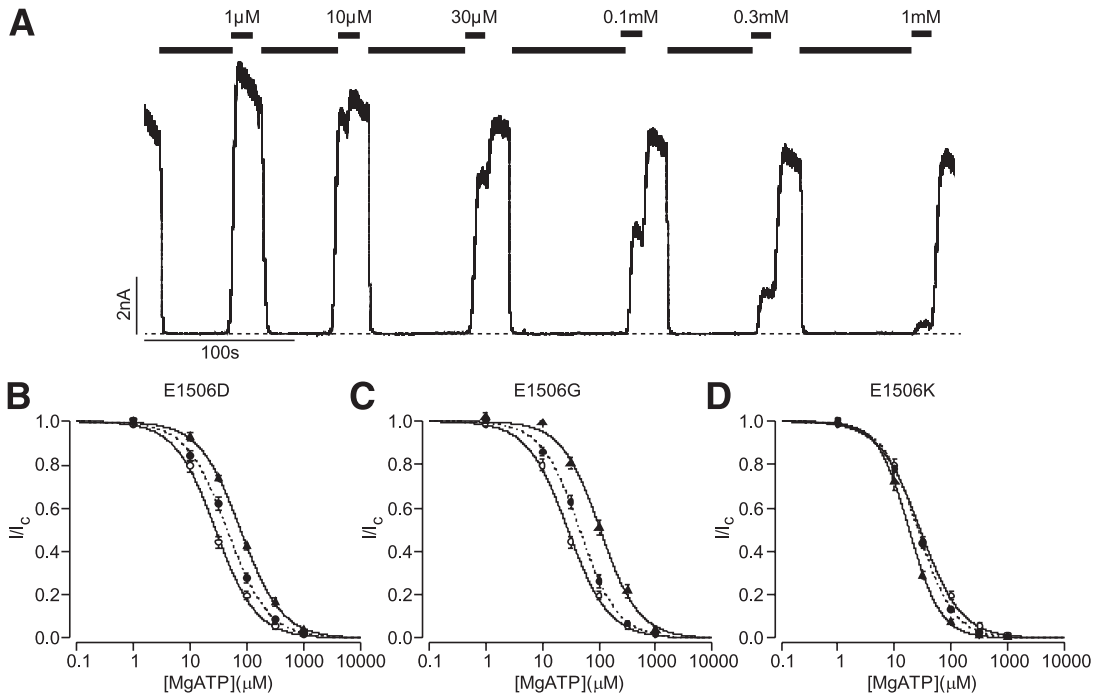

FIG. 6. ATP sensitivity of wild-type and mutant channels after preconditioning with 10 mmol/L MgATP. *A*: Representative homE1506D currents recorded in response to different MgATP concentrations (as indicated), preceded by a preconditioning pulse in 10 mmol/L MgATP solution (indicated by the unlabeled solid line [——]) and followed by control (nucleotide-free) solution. The dashed lines (- - -) indicate the zero current. *B–D*: Mean relationship between MgATP concentration and K_{ATP} current (I), expressed relative to that in the absence of nucleotide (I_c), after 30-s preincubation in 10 mmol/L MgATP for WT (○, *n* = 9), heterozygous (●), and homomeric mutant (▲) channels. Channels were composed of Kir6.2 and wild-type or mutant SUR1 subunits, as indicated. *B*: homE1506D (*n* = 8), hetE1506D (*n* = 9). *C*: homE1506G (*n* = 7), hetE1506G (n = 7). *D*: homE1506K (*n* = 7), hetE1506K (*n* = 5). The lines are drawn to eq. 1, with the following parameters (in μmol/L for IC_{50}): wild-type, IC_{50} = 28, *h* = 1.2; homE1506D, IC_{50} = 78, *h* = 1.2; hetE1506D, IC_{50} = 45, *h* = 1.2; homE1506G, IC_{50} = 105, *h* = 1.3; hetE1506G, IC_{50} = 45, *h* = 1.3; homE1506K, IC_{50} = 18, *h* = 1.6; hetE1506K, IC_{50} = 26, *h* = 1.4.

abolished, with all three channels showing an ~1.5-fold increase in current in 100 μmol/L MgADP. Interestingly, although MgATP (100 μmol/L) activated G334D/E1506 channels about as effectively as MgADP (100 μmol/L), it was far more effective than MgADP at stimulating all three double-mutant channels; MgATP increased the mutant currents ~3-fold compared with 1.5-fold for MgADP (Fig. 4*C*, Supplementary Fig. 1). The difference in the extent of activation of wild-type and neonatal diabetes channels was not significant.

The time course of channel activation by MgATP and MgADP was also affected by mutations at E1506 of SUR1. Activation of G334D/E1506 channels could be fitted by one exponential with a time constant (τ_{on}) of ~1 s for MgADP and 2.5 s for MgATP (Fig. 5*A* and *B*). In contrast, the time constant of activation by both MgADP and MgATP was increased to ~20 s for all three SUR1 mutant channels.

The time constant of deactivation (τ_{off}) for the G334D/E1506 channels was ~3 s for MgADP and ~5 s for MgATP (Fig. 5*C* and *D*). The off-rate of MgADP was not significantly different for the G334D/E1506K channels but was slower for the G334D/E1506D and G334D/E1506G channels, with a τ_{off} of 10 and 11 s, respectively. The off-rate of MgATP was significantly less for all three mutant channels, with a τ_{off} of 8.5 s for G334D/E1506K, 16 s for G334D/E1506G, and 67 s for G334D/E1506D.

Effects on MgATP activation of the K_{ATP} channel. These results suggest that MgATP is far more efficient than MgADP at activating the E1506 mutant channels. We explored this possibility further using channels composed of wild-type Kir6.2 and wild-type or mutant SUR1. We measured the ATP concentration-inhibition curve after a 30-s exposure to 10 mmol/L MgATP (Fig. 6). Such ATP preconditioning reduced the ATP sensitivity of the two neonatal diabetic mutant channels but had little or no effect on wild-type or E1506K channels, respectively (Table 1). As a consequence, the IC_{50} for the ATP block of the homomeric and heterozygous E1506D and E1506G channels was significantly greater than wild-type, whereas that of hetE1506K was no different, and that of homE1506K was actually slightly smaller (Fig. 6, Table 1). The effect of MgATP preconditioning was dose-dependent (Fig. 7). Preconditioning pulses of >300 μmol/L MgATP markedly reduced the ability of 100 μmol/L MgATP to block E1506D and E1506G channels but had only a small effect on wild-type channels and no effect on the homE1506K channels.

Pre-exposure to 10 mmol/L MgADP, which fully blocked the wild-type and mutant channels, did not affect the ability of 100 μmol/L MgATP to block any of the four channel types (data not shown).

DISCUSSION

Our results provide a functional explanation for why mutation of E1506 in SUR1 to lysine (K) results in hyperinsulinism, whereas mutation of the same residue to aspartate (D) or glycine (G) causes neonatal diabetes. This occurs because the mutations have opposite effects on the whole-cell K_{ATP} currents; hetE1506D and hetE1506G increase resting whole-cell currents, whereas the hetE1506K channels show no resting whole-cell currents and are

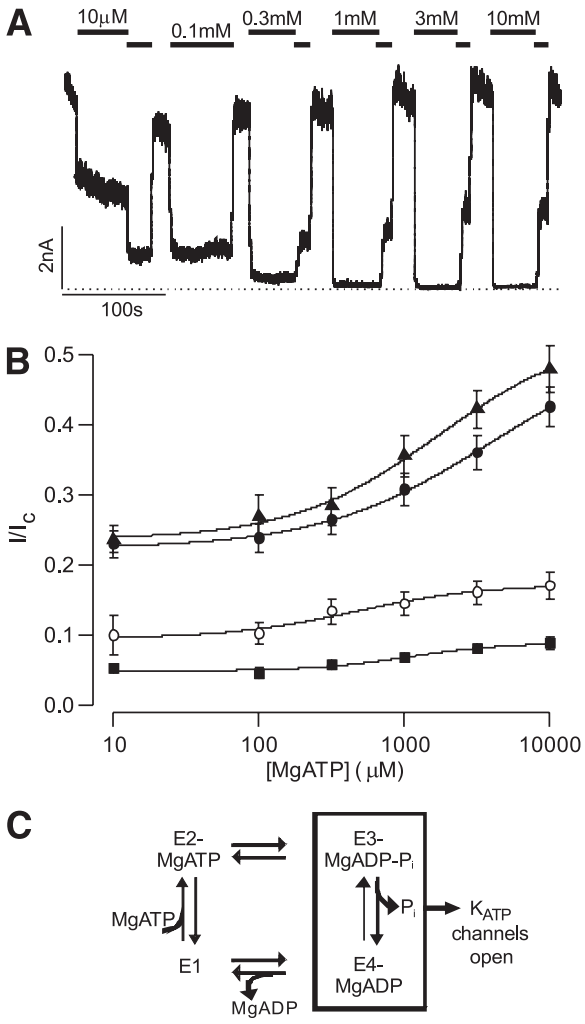

FIG. 7. Concentration dependence of MgATP preconditioning on K_{ATP} channel ATP sensitivity. *A*: Representative homE1506G currents recorded in response to test pulses of 100 μmol/L MgATP (unlabeled solid line [——]), preceded by a preconditioning pulse to a variable MgATP concentration (10 μmol/L to 10 mmol/L, as indicated) and followed by control (nucleotide-free) solution. *B*: MgATP concentration during the conditioning prepulse plotted against the current during a 100 μmol/L MgATP test pulse. Current is expressed as a fraction of that in control (nucleotide-free) solution after the test pulse for wild-type (○, *n* = 14), homE1506D (●, *n* = 15), homE1506G (▲, *n* = 10), and homE1506K (■, *n* = 8) channels. The lines are drawn through the points by eye. The error bars show the SEM. *C*: The SUR1 ATPase catalytic cycle.

activated less in response to metabolic inhibition. An increase in the resting β-cell K_{ATP} current would be expected to produce β-cell hyperpolarization and reduce Ca^{2+} influx and insulin secretion evoked by glucose, thereby predisposing to diabetes. In contrast, a reduction in K_{ATP} current will cause depolarization, maintained Ca^{2+} influx, and persistent insulin secretion, giving rise to hyperinsulinism.

As reported for most other neonatal diabetes mutations in SUR1 (18,21), the increase in the resting whole-cell currents was relatively small. Such small changes are consistent with the relatively mild, transient form of diabetes and the absence of neurological symptoms (6,18). Resting currents in the pancreatic β-cell are likely larger than those measured in the oocyte, perhaps because of lower ATP levels. It is not evident why the diabetes remits, but as is the case for other SUR1 mutations causing transient neonatal diabetes (29), it seems likely the diabetes may later relapse and patients should be monitored for this possibility.

Sulfonylureas are an effective therapy for most patients with neonatal diabetes caused by K_{ATP} channel mutations and are now the treatment of choice for this disease (24). We observed that tolbutamide blocked hetE1506D and hetE1506G currents as much as wild-type K_{ATP} channels, which explains why our patients could be successfully treated with glibenclamide.

Effects of mutations on whole-cell currents. So why does the mutation of E1506 to K abolish resting whole-cell K_{ATP} currents, whereas the mutation to E and G enhances them? We favor the idea that this reflects differences in the channel sensitivity to MgATP. We observed that the neonatal diabetic mutant channels are substantially less sensitive to ATP inhibition if they have been previously exposed to physiological ATP concentrations of 1–10 mmol/L (37). In contrast, this effect was very small for wild-type channels and absent for E1506K channels. These results are consistent with the differences in the resting whole-cell current amplitude we measured in intact oocytes and suggest that neonatal diabetic channels have larger resting currents because they are less sensitive to ATP.

Metabolic inhibition will result in a fall in ATP and an increase in MgADP, both of which will affect the response of the K_{ATP} channel. Both reduced ATP inhibition at Kir6.2 and increased MgADP activation at SUR1 will contribute to the increase in wild-type current and, to a lesser extent, the heterozygous channels. The impaired response of the homE1506K channels may be explained by their markedly reduced MgADP activation, as previously suggested (27). We suggest the small increase in the homE1506D and homE1506G currents is because their reduced MgADP activation is outweighed by their greatly reduced ATP sensitivity, allowing the channels to open in response to falling ATP levels.

Molecular mechanism. Because ATP sensitivity did not change in the absence of Mg^{2+}, it appears that the mutations do not reduce nucleotide block at Kir6.2. Rather, they influence the interaction of Mg-nucleotides with SUR1. E1506 lies within NBS2 of SUR1, close to the γ-phosphate of ATP and its associated Mg^{2+} atom (38). The equivalent residue in other ABC transporters is known to be involved in nucleotide binding and ATPase hydrolysis (32) and its mutation to aspartate dramatically reduces ATPase activity and the initial P (Pi) release in ABC proteins (39,40). Thus mutation of E1506 in SUR1 is likely to alter the conformation that Mg^{2+} nucleotides adopt in the NBS and thereby impair *1*) nucleotide binding, and/or *2*) ATPase activity, and/or *3*) the mechanism by which MgADP occupation at NBS2 is translated into channel opening.

It seems possible that the E1506 mutations trap NBS2 in different conformational states of the ATPase cycle (Fig. 7*C*) that either promote channel activity (E, G) or do not (K). All three mutations markedly reduce MgADP activation of the channel, arguing that occupancy of this state is reduced and/or the translation of the MgADP-bound state into channel activity is impaired. Mutation of the equivalent residue in MRP1 to aspartate does not alter MgADP binding (32), which suggests that SUR1-E1506D might bind MgADP but that binding no longer leads to channel activation.

All mutations support MgATP activation of the channel, as indicated by the use of a Kir6.2 ATP-insensitive mutation. This suggests that MgATP binding/activation are relatively

unaffected. It is not possible to distinguish whether the channel is activated by occupancy of the MgATP-bound state or the MgADP + P_i state, or both (Fig. 7*C*). Nevertheless, the ability of MgATP, but not MgADP, to stimulate mutant channels almost as effectively as wild-type channels argues that one or both of these states can do so. The slower off-rate of MgATP seen with the neonatal diabetes mutations (especially E1506D) may indicate that the channel becomes trapped in a particular state of the reaction cycle that is associated with increased channel activity; for example, the MgATP-bound or MgADP + P_i state. The off-rate of MgADP was much faster than that of MgATP for the E1506D channels, and MgADP had little stimulatory effect, which supports arguments that it cannot be the MgADP-bound state.

The most striking difference between the E1506K and E1506G/E1506D channels is that shown in Figs. 6 and 7: preexposure to millimolar concentrations of MgATP desensitizes the channel to subsequent inhibition by a lower ATP concentration. This cannot be due to an effect of MgATP on kinases, for example, because this should be similar for all channels. There are two obvious possibilities.

First, exposure to a saturating ATP concentration for an extended period may force the channels into a state in which NBS1 and NBS2 on all four subunits are both occupied by nucleotide, and this may lead to greater channel activation. Second, it may relate to the slower off-rate of MgATP of neonatal diabetes channels, which could maintain the channel in an activated state for an extended period, so impairing ATP block. As shown previously, Mg-nucleotide activation not only enhances channel activity per se but also reduces ATP inhibition at Kir6.2 (41). In the β-cell, where ATP levels are normally within the millimolar range, this mechanism would result in reduced ATP inhibition and thus larger resting K_{ATP} currents.

ACKNOWLEDGMENTS

This work was supported by Wellcome Trust (076436/Z/05/Z and 081188/A/06/Z), the Royal Society, and the European Union (EuroDia-[LSHM-CT-2006-518153]). S.E.F. is the Sir Graham Wilkins, Peninsula Medical School Research Fellow, and F.M.A. is a Royal Society Research Professor.

No potential conflicts of interest relevant to this article were reported.

R.M. researched electrophysiology data, contributed to discussion, and reviewed the manuscript. S.E.F. researched molecular genetics data, contributed to discussion, and reviewed the manuscript. X.S. researched electrophysiology data, contributed to discussion, and reviewed the manuscript. D.S. and K.H. identified the patients, contributed to discussion, and reviewed the manuscript. S.E. and A.T.H. directed the research, contributed to discussion, and reviewed the manuscript. F.M.A. directed the research, contributed to discussion, wrote the manuscript, and reviewed the manuscript.

REFERENCES

1. Nichols CG. K_{ATP} channels as molecular sensors of cellular metabolism. Nature 2006;440:470–476
2. Miki T, Seino S. Roles of K_{ATP} channels as metabolic sensors in acute metabolic changes. J Mol Cell Cardiol 2005;38:917–925
3. Ashcroft FM. The Walter B. Cannon Physiology in Perspective Lecture, 2007. ATP-sensitive K^+ channels and disease: from molecule to malady. Am J Physiol Endocrinol Metab 2007;293:E880–E889
4. Ashcroft FM, Harrison DE, Ashcroft SJH. Glucose induces closure of single potassium channels in isolated rat pancreatic β-cells. Nature 1984;312:446–448
5. Gloyn AL, Pearson ER, Antcliff JF, et al. Activating mutations in the gene encoding the ATP-sensitive potassium-channel subunit Kir6.2 and permanent neonatal diabetes. N Engl J Med 2004;350:1838–1849
6. Hattersley AT, Ashcroft FM. Activating mutations in Kir6.2 and neonatal diabetes: new clinical syndromes, new scientific insights, and new therapy. Diabetes 2005;54:2503–2513
7. Flanagan SE, Patch AM, Mackay DJ, et al. Mutations in ATP-sensitive K^+ channel genes cause transient neonatal diabetes and permanent diabetes in childhood or adulthood. Diabetes 2007;56:1930–1937
8. De León DD, Stanley CA. Mechanisms of disease: advances in diagnosis and treatment of hyperinsulinism in neonates. Nat Clin Pract Endocrinol Metab 2007;3:57–68
9. Pinney SE, MacMullen C, Becker S, et al. Clinical characteristics and biochemical mechanisms of congenital hyperinsulinism associated with dominant K_{ATP} channel mutations. J Clin Invest 2008;118:2877–2886
10. Koster JC, Marshall BA, Ensor N, Corbett JA, Nichols CG. Targeted overactivity of beta cell K_{ATP} channels induces profound neonatal diabetes. Cell 2000;100:645–654
11. Girard CA, Wunderlich FT, Shimomura K, et al. Expression of an activating mutation in the gene encoding the K_{ATP} channel subunit Kir6.2 in mouse pancreatic β cells recapitulates neonatal diabetes. J Clin Invest 2009;119:80–90
12. Clement JP 4th, Kunjilwar K, Gonzalez G, et al. Association and stoichiometry of $K_{(ATP)}$ channel subunits. Neuron 1997;18:827–838
13. Mikhailov MV, Campbell JD, de Wet H, et al. 3-D structural and functional characterization of the purified K_{ATP} channel complex Kir6.2-SUR1. EMBO J 2005;24:4166–4175
14. Nichols CG, Shyng SL, Nestorowicz A, et al. Adenosine diphosphate as an intracellular regulator of insulin secretion. Science 1996;272:1785–1787
15. Tucker SJ, Gribble FM, Zhao C, Trapp S, Ashcroft FM. Truncation of Kir6.2 produces ATP-sensitive K^+ channels in the absence of the sulphonylurea receptor. Nature 1997;387:179–183
16. Gribble FM, Tucker SJ, Ashcroft FM. The essential role of the Walker A motifs of SUR1 in K_{ATP} channel activation by Mg-ADP and diazoxide. EMBO J 1997;16:1145–1152
17. Shyng S, Ferrigni T, Nichols CG. Regulation of K_{ATP} channel activity by diazoxide and MgADP. Distinct functions of the two nucleotide binding folds of the sulfonylurea receptor. J Gen Physiol 1997;110:643–654
18. McTaggart JS, Clark RH, Ashcroft FM. The role of the K_{ATP} channel in glucose homeostasis in health and disease: more than meets the islet. J Physiol 2010;588:3201–3209
19. Babenko AP, Polak M, Cavé H, et al. Activating mutations in the *ABCC8* gene in neonatal diabetes mellitus. N Engl J Med 2006;355:456–466
20. Proks P, Shimomura K, Craig TJ, Girard CA, Ashcroft FM. Mechanism of action of a sulphonylurea receptor SUR1 mutation (F132L) that causes DEND syndrome. Hum Mol Genet 2007;16:2011–2019
21. de Wet H, Proks P, Lafond M, et al. A mutation (R826W) in nucleotide-binding domain 1 of *ABCC8* reduces ATPase activity and causes transient neonatal diabetes. EMBO Rep 2008;9:648–654
22. Koster JC, Cadario F, Peruzzi C, Colombo C, Nichols CG, Barbetti F. The G53D mutation in Kir6.2 (*KCNJ11*) is associated with neonatal diabetes and motor dysfunction in adulthood that is improved with sulfonylurea therapy. J Clin Endocrinol Metab 2008;93:1054–1061
23. Gribble FM, Reimann F. Sulphonylurea action revisited: the post-cloning era. Diabetologia 2003;46:875–891
24. Pearson ER, Flechtner I, Njølståd PR, et al.; Neonatal Diabetes International Collaborative Group. Switching from insulin to oral sulfonylureas patients with diabetes due to Kir6.2 mutations. N Engl J Med 2006;355:467–477
25. Ashcroft FM. New uses for old drugs: neonatal diabetes and sulphonylureas. Cell Metab 2010;11:179–181
26. Huopio H, Otonkoski T, Vauhkonen I, Reimann F, Ashcroft FM, Laakso M. A new subtype of autosomal dominant diabetes attributable to a mutation in the gene for sulfonylurea receptor 1. Lancet 2003;361:301–307
27. Huopio H, Reimann F, Ashfield R, et al. Dominantly inherited diazoxide-responsive form of hyperinsulinism caused by a sulfonylurea receptor 1 mutation. J Clin Invest 2000;106:897–906
28. Aguilar-Bryan L, Nichols CG, Wechsler SW, et al. Cloning of the beta cell high-affinity sulfonylurea receptor: a regulator of insulin secretion. Science 1995;268:423–426
29. Aittoniemi J, Fotinou C, Craig TJ, de Wet H, Proks P, Ashcroft FM. SUR1: a unique ABC protein that functions as an ion channel regulator. Philos Trans R Soc Lond B Biol Sci 2009;364:257–267

30. Matsuo M, Tanabe K, Kioka N, Amachi T, Ueda K. Different binding properties and affinities for ATP and ADP among sulfonylurea receptor subtypes, SUR1, SUR2A, and SUR2B. J Biol Chem 2000;275:28757–28763
31. Zingman LV, Alekseev AE, Bienengraeber M, et al. Signaling in channel/enzyme multimers: ATPase transitions in SUR module gate ATP-sensitive K^+ conductance. Neuron 2001;31:233–245
32. Payen LF, Gao M, Westlake CJ, Cole SPC, Deeley RG. Role of carboxylate residues adjacent to the conserved core Walker B motifs in the catalytic cycle of multidrug resistance protein 1 (*ABCC1*). J Biol Chem 2003;278:38537–38547
33. Gribble FM, Ashfield R, Ammälä C, Ashcroft FM. Properties of cloned ATP-sensitive K^+ currents expressed in Xenopus oocytes. J Physiol 1997;498:87–98
34. Gribble FM, Tucker SJ, Haug T, Ashcroft FM. MgATP activates the β cell K_{ATP} channel by interaction with its SUR1 subunit. Proc Natl Acad Sci U S A 1998;95:7185–7190
35. Ohno-Shosaku T, Zünkler BJ, Trube G. Dual effects of ATP on K^+ currents of mouse pancreatic beta-cells. Pflugers Arch 1987;408:133–138
36. Drain P, Li L, Wang J. K_{ATP} channel inhibition by ATP requires distinct functional domains of the cytoplasmic C terminus of the pore-forming subunit. Proc Natl Acad Sci U S A 1998;95:13953–13958
37. Gribble FM, Loussouarn G, Tucker SJ, Zhao C, Nichols CG, Ashcroft FM. A novel method for measurement of submembrane ATP concentration. J Biol Chem 2000;275:30046–30049
38. Campbell JD, Sansom M, Ashcroft FM. Potassium channel regulation. Structural insights into the function of the nucleotide-binding domains of the human sulphonylurea receptor. EMBO Rep 2003;4:1038–1042
39. Carrier I, Gros P. Investigating the role of the invariant carboxylate residues E552 and E1197 in the catalytic activity of Abcb1a (mouse Mdr3). FEBS J 2008;275:3312–3324
40. Tombline G, Bartholomew LA, Tyndall GA, Gimi K, Urbatsch IL, Senior AE. Properties of P-glycoprotein with mutations in the "catalytic carboxylate" glutamate residues. J Biol Chem 2004;279:46518–46526
41. Proks P, de Wet H, Ashcroft FM. Activation of the K_{ATP} channel by Mg-nucleotide interaction with SUR1. J Gen Physiol 2010;136:389–405